6. SITE 669[1]

Shipboard Scientific Party[2]

HOLE 669A

Date occupied: 31 May 1986, 0815L

Date departed: 2 June 1986, 0500L

Time on hole: 1 day, 20 hr, 45 min (includes television-sonar survey time)

Position: 23°31.02'N, 45°02.75'W

Water depth (sea level; corrected m; echo-sounding): 1971.2

Water depth (rig floor; corrected m; echo-sounding): 1982.3

Bottom felt (m, drill pipe): 1979

Distance between rig floor and sea level (m): 11.1

Total depth (rig floor; m): 1983

Penetration (m): 4.0

Number of cores: 1

Total length of cored section (m): 4.0

Total core recovered (m): 0.10

Core recovery (%): 2.5

Sediment: basalt rubble with intermixed sediment

Basement:

Depth sub-bottom (m): approximately 4 m (resistance to drilling increased markedly at approximately 4 mbsf, interpreted as being the top of the basement).

Nature: unknown—none recovered

Velocity range of basalt rubble (km/s): 5.59

Principal Results: *JOIDES Resolution* occupied Site 669 from 31 May to 2 June 1986 and drilled in a water depth of 1979 m. The site was chosen on top of a hill at 23°31.02'N, 45°02.75'W, on the western flank of the rift valley and southwestern slope of the deep, funnel-shaped nodal basin marking the intersection of the median valley and the Kane Fracture Zone. Surface exposures of plutonic rocks, mainly gabbros, had been located in this area during previous ALVIN diving programs.

A site survey was conducted using the television-sonar system, which was run down on the coaxial cable without the drill pipe. The flat bottom appeared to be covered with basaltic rubble and sediment. We then spudded-in Hole 669 successfully, using a positive displacement coring motor (PDCM). Drilling progress was monitored by the television-sonar system, which had been run back down on the drill string. Four meters of penetration were realized rapidly. At this point, the penetration rate fell off dramatically, probably indicating that the gabbro basement had been reached. Despite an increase in the flow rate through the motors and an increase in the weight run on the bit, the PDCM continually stalled. Moreover, a large piece of rubble became jammed in the core catcher, preventing retrieval. Drilling operations at Site 669A were then suspended.

We penetrated a total of 4 m in Hole 669A and recovered 0.1 m of core (two pieces of basalt from the rubble cover). The two pieces of aphyric basalt are tholeiitic basalts, similar to some of the olivine phyric basalts collected from the walls of the Kane Fracture Zone, and show evidence of incipient alteration characterized by the "dark halos" stage (mainly orange smectites, green to yellow clays, and iron hydroxyoxides). Aragonite crystals were found in some vesicles and miaroles.

BACKGROUND AND OBJECTIVES

One of the main goals of Leg 109 was testing the feasibility of unsupported spud-in and coring in exposed plutonic rock outcrops in the Kane Fracture Zone area. The success of such a test could have important consequences on the future of drilling plans in this difficult environment.

The ALVIN diving program in 1980 (Karson and Dick, 1983) and the Sea Beam map of Detrick et al. (1985) provided the survey data used for site selection. Exposures of plutonic rocks had been located on the western flank of the rift valley and southwestern slope of the deep, funnel-shaped nodal basin marking the intersection of the median valley and the Kane Fracture Zone (Fig. 1). The nodal basin, which is >6000 m below sea level (mbsl), was ruled out as a possible site because it would be time consuming for the pipe runs, unsafe for the television-sonar system, and probably difficult to drill because of a large thickness of rubble. To minimize these problems, we chose the top of a hill at 23°31.02'N, 45°02.75'W for the following reasons: (1) during ALVIN dive number 1012, plutonic gabbros were observed and sampled along small scarps in several places on the flanks of the hill; (2) its flat surface and shallow depth, nearly 2000 mbsl, were thought to be adequate for spudding-in, which would facilitate short pipe runs; and (3) this topographic high is the dominant elevation of the whole area, so that the rubble thickness should logically be at a minimum.

With these criteria in mind, we selected Site 669, located on a flat area just on the southeastern flank of the hill, at the 2000-m isobath on the Sea Beam map (Fig. 2). Our scientific and engineering objectives were to try spudding-in over a basement outcrop and to use the PDCM to establish and core a hole in gabbroic plutonic rock. We expected the core to yield important in-

---

[1] Shipboard Scientific Party, 1988. *Proc. ODP, Init. Repts. (Pt. A)*, 109: College Station, TX (Ocean Drilling Program).

[2] Wilfred B. Bryan (Co-Chief Scientist), Department of Geology and Geophysics, Woods Hole Oceanographic Institution, Woods Hole, MA 02543; Thierry Juteau (Co-Chief Scientist), Laboratoire de Pétrologie, Université de Bretagne Occidentale, 6 Avenue Le Gorgeu, 29287 Brest, France; Andrew C. Adamson (ODP Staff Scientist), Ocean Drilling Program, Texas A&M University, College Station, TX 77843; Laurie K. Autio, Deptartment of Geology and Geography, Morrill Science Center, University of Massachusetts, Amherst, MA 01003; Keir Becker, R.S.M.A.S., Division of Marine Geology and Geophysics, University of Miami, 4600 Rickenbacker Causeway, Miami, FL 33149; M. Mansour Bina, Laboratoire de Géomagnetisme, Université Pierre et Marie Curie, 4, Avenue de Neptune, 94107 St. Maur des Fosses, France; Jean-Philippe Eissen, O.R.S.T.O.M., B.P. A5, Noumea, New Caledonia (current address: O.R.S.T.O.M., IFREMER, BP 337, 2273 Brest Cedex, France); Toshitsugu Fujii, Earthquake Research Institute, University of Tokyo, 1-1-1 Yayoi, Bunkyo-ku, Tokyo 113, Japan; Timothy L. Grove, Department of Earth, Atmospheric and Planetary Sciences, Massachusetts Institute of Technology, Cambridge, MA 02139; Yozo Hamano, Earthquake Research Institute, University of Tokyo, 1-1-1 Yayoi, Bunkyo-ku, Tokyo 113, Japan; Rejean Hebert, Departement de Géologie, Université Laval, Quebec G1K 7P4, Canada; Stephen C. Komor, Bureau of Mines, Avondale Research Center, 4900 LaSalle Road, Avondale, MD 20782 (current address: Department of Geology and Geophysics, University of Wisconsin, Madison, WI 53706); Johannes Kopietz, Bundesanstalt für Geowissenschaften und Rohstoffe, Stilleweg 2, D-3000 Hannover 51, Federal Republic of Germany; Kristian Krammer, Institut für Geophysik, Universität München, Theresienstrasse 41, D-8000 München 2, Federal Republic of Germany; Michel Loubet, Laboratoire de Mineralogie, Université Paul Sabatier, 38 Rue des 36 Ponts, 31400 Toulouse, France; Daniel Moos, Borehole Research Group, Lamont-Doherty Geological Observatory, Columbia University, Palisades, NY 10964; Hugh G. Richards, Department of Geology, The University, Newcastle upon Tyne NE1 7RU, United Kingdom.

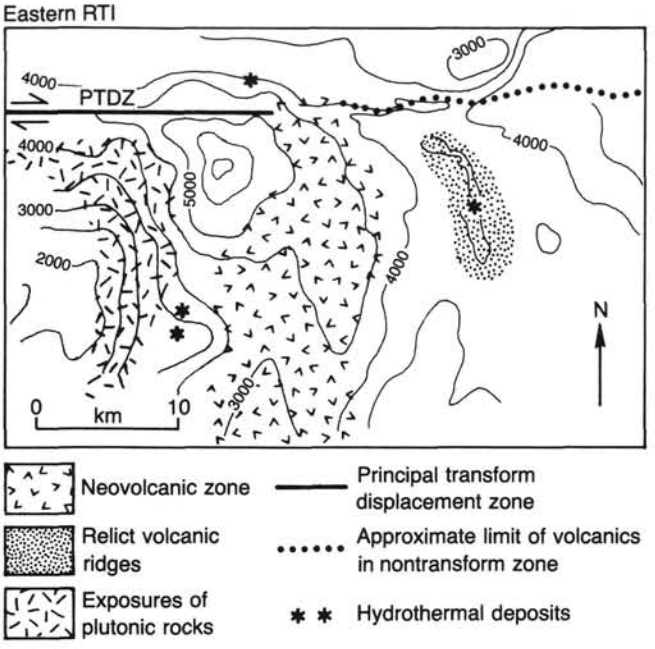

Figure 1. Map of intersection of median valley with Kane Fracture Zone at about 23°30'N, 45°00'W. RTI = ridge/transform intersection; PTDZ = principal transform displacement zone. After Karson and Dick (1983).

formation on mineralogic layering and tectonic deformation in the gabbro.

OPERATIONS

Coring with an Unsupported Bottom-Hole Assembly

A preliminary site survey, conducted using the television-sonar system run down on the coaxial cable without the drill pipe, showed that the bottom had little or no relief and was covered with sediment. A drill site was selected that consisted of sediment and rubble appearing to be cemented together. We hoped that the surface materials would be sufficiently consolidated to provide limited bit confinement while spudding-in. A sonar reflector was released from the television-sonar system at the desired drill site.

Upon completion of the site survey, the television-sonar system was pulled back to the surface and the PDCM drilling assembly was lowered on the drill string, fitted with a 10.5-in. × 2.25-in. core bit having a type 9 conical cutting structure. The television-sonar system was then run back down on the drill pipe to locate the drill site.

The bit was positioned 3–4 m from the buoyed sonar reflector. Using the television-sonar system to monitor drilling operations, we tagged the seafloor at 1979 m below rig floor and spudded in the hole successfully. Owing to the lack of consolidation of the upper sediments, 2–3 m of penetration were realized rapidly. The hole was spudded-in with a 0–4000-lb weight on the bit, a 260-gal/min flow through the motor, a 300-psi stand-pipe pressure, and a 40–50-RPM bit rotation.

We progressed to a depth of 4 mbsf, where the penetration rate fell off dramatically, probably indicating that the underlying gabbro basement had been reached. The flow rates through the motor were increased to 570 gal/min, resulting in rotational speeds of 90 RPM. We attempted to increase the weight on the bit, which, however, resulted in the continual stalling out of the motor. A maximum of a 4000-lb weight on the bit could be run while still maintaining effective bit rotation. The bit appeared to skid on the gabbro rather than to penetrate it.

Because of the poor penetration rate, we pulled the bit out of the hole. We planned to offset 100 m in hopes of finding a more desirable drilling location; however, we encountered difficulties while attempting to retrieve the core barrel. After making three unsuccessful attempts to retrieve the barrel, we tripped the drilling assembly out of the hole. A large piece of rubble, jammed in the core catcher and throat of the bit, had induced a torsional load on the core-barrel system, which resulted in torsional failure of the threaded connection between the two 15-ft core-barrel sections. The induced torsional load also backed off several other core-barrel system connections to varying degrees.

We suspended drilling operations at Hole 669A because of lack of basement penetration and mechanical problems with the PDCM. A total of 4-m penetration was made in Hole 669A and 0.1 m of core was recovered (Table 1). While in transit to Hole 395A, we made repairs to the coring motor, readying it for use later in the leg.

LITHOSTRATIGRAPHY

We drilled Hole 669A through 4.0 m of intermixed sediment and basalt rubble overlying presumed gabbroic basement rock. Drilling became substantially more difficult at 4.0 mbsf, when the coring motor began to stall out; this point is interpreted as marking the top of the underlying basement. We recovered 0.1 m of aphyric basalt rubble, equivalent to a recovery rate of 2.5%. The nature of the basement remains unknown.

PETROGRAPHY

Drilling operations at site 669A recovered two pieces of macroscopically aphyric basalt. Only one plagioclase phenocryst is visible in Sample 109-669A-1D-1, 11–13 cm. Vesicles (0.2–1.0 mm) are round and either empty, partly filled with microcrystalline groundmass, or lined by secondary minerals. Irregularly shaped miaroles are also partly filled by secondary minerals.

One thin section of Sample 109-669A-1D-1, 7–9 cm, and two thin sections of Sample 109-669A-1D-1, 11–13 cm, were prepared. The basalts are predominantly fresh with <2%–4% alteration products, except in the marginal halos (see "Alteration" section, this chapter). The groundmass texture in both thin sections of Sample 109-669A-1D-1, 11–13 cm, varies from spherulitic-subvariolitic to felty (microcrystalline intergranular texture; average diameter, 0.1 mm; MacKenzie et al., 1982; Fig. 3), whereas it is subvariolitic to microlitic and coarser grained (average diameter, 0.2 mm) in Sample 109-669A-1D-1, 7–9 cm, thin section. The mode contains as much as 0.6% olivine phenocrysts (Table 2), which are isolated or in clusters. Individual olivine phenocrysts (0.2–0.6 mm) are euhedral to anhedral, and some contain light-brown devitrified glass and colorless bubble-containing nondevitrified glass inclusions (Fig. 4). The groundmass in both samples is composed of plagioclase-clinopyroxene and clinopyroxene spherulites, olivine microphenocrysts, and mesostasis. The mesostasis (20%–24% in fine-grained samples, 54% in the coarser grained Sample 109-669A-1D-1, 7–9 cm) consists of plagioclase and clinopyroxene microlites, interstitial glass, and opaque minerals. The opaque minerals are dendritic titanomagnetite, needlelike ilmenite (only in Sample 109-669A-1D-1, 7–9 cm, thin section), and sulfide, listed in order of decreasing abundances. The spherulites and variolelike microstructures (0.5–1.2 mm) are formed by acicular plagioclase (0.1–0.6 mm in diameter but as much as 2 mm in length in Sample 109-669A-1D-1, 7–9 cm), and bladed clinopyroxene (0.1–0.4 mm), radiating from nuclei of plagioclase. Olivine microphenocrysts (<0.1 mm in Sample 109-669A-1D-1, 11–13 cm, <0.2 mm in Sample 109-669A-1D-1, 7–9 cm) exhibit quenched morphology similar to the swallowtail shapes described by Bryan (1972) and are attached to plagioclase microlites. Olivine microphenocrysts account for 2.6%–6% of the groundmass. Plagioclase (0.05–0.6

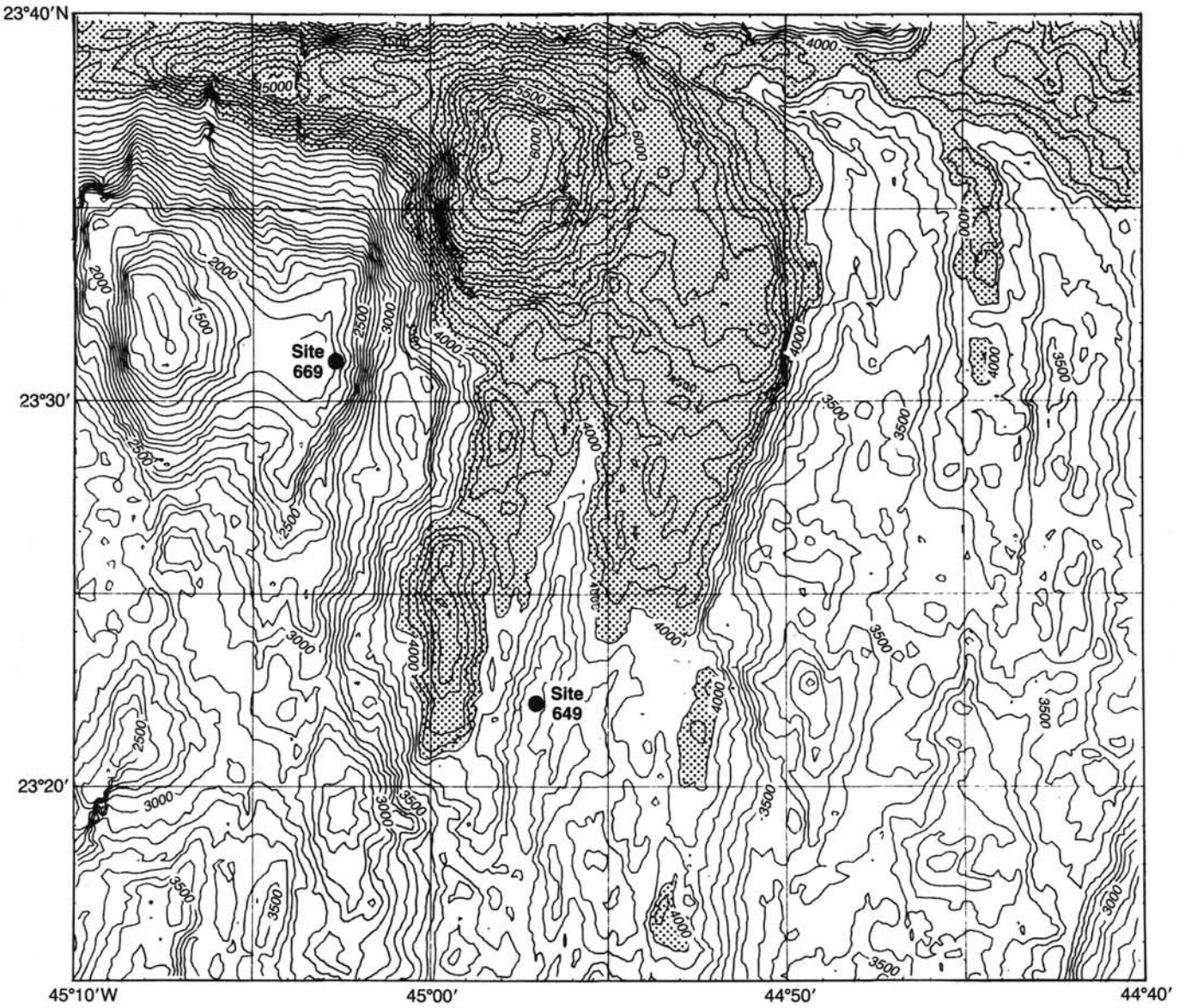

Figure 2. Detailed bathymetry around Site 669. Depths >4000 m are shaded. Sea Beam map after Detrick et al. (1985).

Table 1. Coring summary, Site 669.

Core no.	Date (June 1986)	Time on deck	Total depth (m) top	Total depth (m) bottom	Sub-bottom depths (m)	Advanced (m)	Length cored (m)	Length recovered (m)	Recovery (%)
Hole 669A									
109-669A-1D	2	0200	1979	1983	0.0–4.0	4.0	4.0	0.10	2.5

mm wide) is acicular to hopper shaped and is found as bundles or in close association with clinopyroxene as spherulites (Figs. 5 and 6). Plagioclase content varies from 26% to 33% of the groundmass. Clinopyroxene (0.1–0.4 mm) is a microcrystalline groundmass phase interpenetrated with plagioclase microlites, and its shape ranges from plumose to arborescent to spherulitic (Fig. 6). Modal groundmass clinopyroxene varies from 32% to 38% in both of the Sample 109-669A-1D-1, 11–13 cm, thin sections.

Spherical segregation vesicles (0.5–1.0 mm) that have been completely filled by residual liquid are also present. The residual liquid has crystallized into a microcrystalline to cryptocrystalline texture and mineral composition, which are both similar to the mesostasis. The clinopyroxene is more arborescent in the vesicles. Sharp color differences between the central part (light brown), the outer rim of the segregation vesicles (dark brown), and the mesostasis (medium dark brown) make them easily recognized.

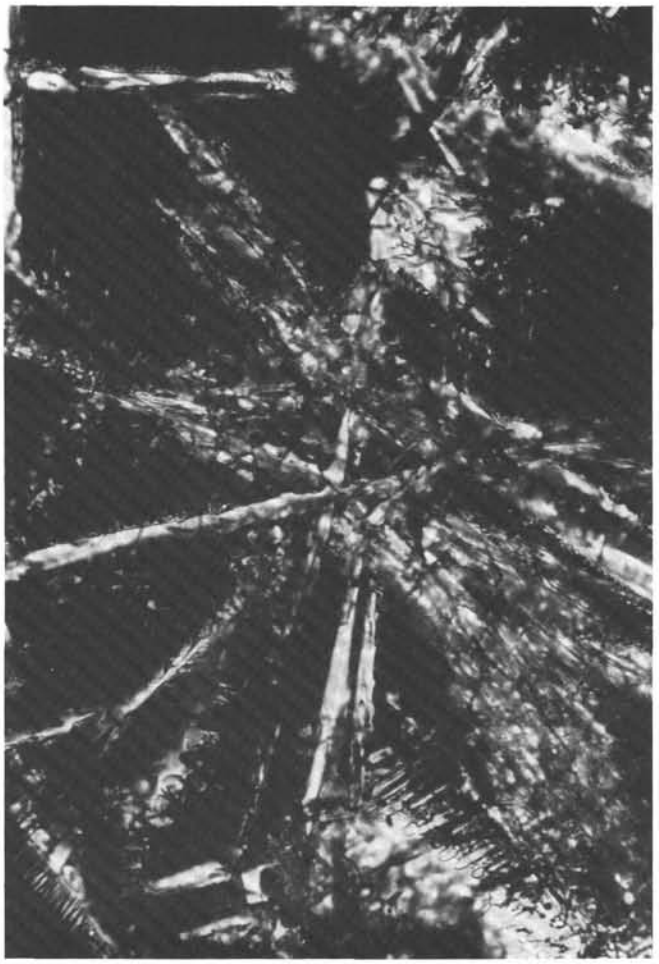

Figure 3. Detail of subvariolitic texture in thin section of Sample 109-669A-1D-1, 11–13 cm, showing radiating clinopyroxene and plagioclase. Field of view = 3 mm.

Figure 4. Olivine phenocryst with glass inclusion in thin section of Sample 109-669A-1D-1, 11–13 cm. Field of view = 3 mm.

Table 2. Modal data, Hole 669A[a].

Sample	Piece no.	Texture[b]	Phenocryst[c,h]	Groundmass[d]						
			Olivine	OL	PLAG	CPX	MESO	[e]OPAQ	GLAS	[f]VES
109-669A-1D-1, 07–09 cm	1	VAR-MIC	Tr	2.6	29.1	10.8	[g]54.0	0.7	—	Tr
109-1D-1, 11–13A	2	SPH-VAR	Tr	6.0	33.1	32.2	24.3	1.5	0.8	2
109-1D-1, 11–13B	2	FEL	0.6	3.6	26.2	38.8	20.9	5.4	0.3	2

[a] Modes are based on 1,000 points counted on 0.5-mm grid spacing. Alteration products are not included in the sums. Vesicles are visual estimates and are not included in the modal sums.
[b] Textural abbreviations are listed in order of predominance in thin sections: SPH: spherulitic; VAR: subvariolitic; FEL: felty; MIC: microlitic.
[c] Phenocryst category includes crystals obviously larger than groundmass phases. Olivine typically is 0.2–0.6 mm in diameter.
[d] OL: olivine; PLAG: plagioclase; CPX: clinopyroxene; MESO: mesostasis; OPAQ: opaques; GLAS: glass (interstitial glass, segregation vesicles, and glass inclusions); VES: vesicles.
[e] General abundance of opaque minerals is titanomagnetite ≫ sulfide. Ilmenite is present only in thin sample of Sample 109-669A-1D-1, 7–9 cm, where it occurs as an intermediate in abundance between titanomagnetite and sulfide.
[f] Includes miaroles that form 25% of all voids.
[g] Includes minute clinopyroxene and plagioclase microlites and cryptocrystalline groundmass.
[h] Occurrence of plagioclase phenocryst is observed on a macroscopic scale only.

Geochemistry

An analysis of Sample 109-669A-1D-1, 11–13 cm (Table 3) shows that it is type I mid-ocean ridge basalt (MORB) (Bryan et al., 1976) with Zr/Nb > 40. This basalt is similar to other relatively high TiO_2 basalts recovered by dredging near the median valley, especially from KNR-79 Station 27 (W. B. Bryan, pers. comm., 1986), and to some basalts drilled during Leg 49 along the Mid-Atlantic Ridge (Tarney et al., 1979). The Hole 669A sample has the same tendency toward relatively high TiO_2 (1.9%) at moderate MgO levels (7.5%) exhibited by basalts from Sites 648 and 649. The trace element abundances reflect a similar dis-

Figure 5. Detail of spherulitic texture in thin section of Sample 109-669A-1D-1,11-13, showing bundles of clinopyroxene and minor amounts of plagioclase in groundmass. Field of view = 2 mm.

Figure 6. Hopper-shaped plagioclase in groundmass in thin section of Sample 109-669A-1D-1, 11-13 cm. Field of view = 3 mm.

position with relatively high abundances of incompatible elements (Zr = 151 ppm, Y = 40 ppm) at moderate levels of compatible elements (e.g., Ni = 96 ppm).

Summary and Conclusions

The very fine-grained spherulitic-subvariolitic to felty-microlitic textures suggest that the recovered samples come from the outer part of a cooling unit (pillow or lava flow) close to the chilled margin. The textures are typical of rapidly cooled lava erupted in undersea conditions. The occurrence of olivine as the main phenocryst phase and the relatively abundant olivine microphenocrysts indicate that these basalts may be similar to other olivine phyric basalt samples collected from the walls of the Kane Fracture Zone (Bryan et al., 1981).

ALTERATION

The two basalt pieces recovered from Site 669 show somewhat different styles of alteration and are thus described separately here. The optical properties of most of the alteration products that occur are described in the "Alteration" section of Site 648 chapter (this volume).

Sample 109-669A-1D-1 (Piece 1, 4–6 cm)

Alteration within the Rock

The sawn surface is bounded on most sides by a dark halo, which is uniformly 4 mm thick, except where truncated by fracture.

Table 3. Whole-rock analyses, Hole 669A.

Hole-core-section-interval analyst[a]	Sample 109-669A-1D-1, 11–13 cm ship
SiO_2	49.56
TiO_2	1.91
Al_2O_3	15.04
[b]Fe_2O_3*	11.96
MnO	0.19
MgO	7.50
CaO	10.69
Na_2O	2.84
K_2O	0.22
P_2O_5	0.19
Total	100.10
[c]Mg′ value	0.580
Rb	1.9
Sr	145
Y	40
Zr	151
Nb	3.4
Ni	96

[a] Analyzed shipboard on Leg 109.
[b] Total Fe analyzed as Fe_2O_3.
[c] Mg′ value calculated from molar (MgO/MgO + FeO), where $Fe^{2+}/(Fe^{3+} + Fe^{2+}) = 0.9$.

tures. A few vesicles in the halo zone are lined with a bluish clay that appears yellow in transmitted light (probably potassium-rich smectite, by comparison to Hole 648B). The interior of the sample is lighter gray.

In thin section, the halo zones are seen to contain about 7% secondary minerals (500 point counts within a halo), of which >5% is yellow birefringent clay. Most of the clay in this sample occurs as nearly complete fillings of miarolitic cavities, from submicroscopic to 3–4 mm in size. Euhedral plagioclase, olivine, and uncommonly large magnetite project into the larger cavities and are overgrown by homogeneously colored botryoidal, locally radiating clay (Fig. 7). Trace amounts of orange-red clay and red (and sometimes opaque) iron-hydroxyoxides occur in some cavities. The typical mineral sequence appears to range from clays to an increasing iron-hydroxyoxide content in the centers of the fillings, where opaque iron-hydroxyoxide may occur. However, in some cavities, small (30–50 μm) blebs of red iron-hydroxyoxide attached to the walls are overgrown by a thin layer of yellow clay. Cracks are common in this sample, locally occurring roughly parallel at about 0.1-mm intervals. The cracks are <5 μm wide and are filled with yellow clay or red iron-hydroxyoxide. In contrast to the miarolitic cavities, the vesicles in the halo zones are mainly empty. A few have yellow clay or red iron-hydroxyoxide linings as much as 50 μm thick. Sulfide globules remain in the halo zones, but they are less abundant than in the lighter gray zone, and the larger (as much as 6 μm) globules seen in the lighter zone are lacking in the halo zones.

The central, lighter gray zone of the sample appears relatively fresh, apart from some pale greenish yellow staining in the miarolitic cavities and the occurrence of radiating acicular aragonite in two irregular vesicles in the working half. In thin section, the greenish yellow staining is seen to be due to miarolitic linings of nonbirefringent yellowish brown "clay" about 10 μm thick. Sparse flecks of orange to red iron-hydroxyoxide occur near the edges of vesicles or on vesicle walls, including the aragonite-containing vesicles. All these vesicles were probably in communication with the halo zones.

Before thin sections were made of aragonite, it was photographed using the SEM (Figs. 8 and 9). The bladed habit of some of the crystals (Fig. 9) differs from the more typical hexagonal prismatic habit of aragonite but is consistent with the orthorhombic symmetry. Optical properties are diagnostic of aragonite. The two prominent aragonite-containing vesicles (Fig. 8) are partly miarolitic, so that hopper-shaped olivine and other euhedral primary minerals occur partly enclosed in aragonite. Aragonite also completely fills smaller miarolitic cavities near one of the halo boundaries.

Alteration Products Coating the Rock

The sample has various coating minerals. The surfaces parallel to which the dark halo developed are heterogeneously coated with a soft, creamy-colored mineral that locally has a crudely tabular habit. This appears to overlie patches of black MnO_2(?). There are also scattered shiny botryoidal protuberances of red iron-hydroxyoxide and black MnO_2(?) or manganese-rich hydroxyoxides ("micromanganese nodules") as large as 0.1 mm.

A second type of coating is a very thin layer of dull olive-green cryptocrystalline clay (smectite?) developed on fracture surfaces that truncate the dark halos. These coatings apparently represent places where the rock was broken by the drilling along clay-filled fractures, whereas the other type of coating represents the weathering surfaces that were exposed on the seafloor.

Sample 109-669A-1D-1 (Piece 2, 10–16 cm)

Alteration within the Rock

The groundmass of most of the sample is altered to a dark gray. Macroscopically visible alteration products are chiefly iron-

Figure 7. Part of miarolitic cavity almost filled with yellow smectite (Sm), showing botryoidal overgrowths of smectite on euhedral primary minerals projecting into the cavity. Sample 109-669A-1D-1, 4–6 cm. Crossed polars.

Figure 8. Radiating aragonite in irregular vesicles. Sample 109-669A-1D-1, 4–6 cm. SEM photograph.

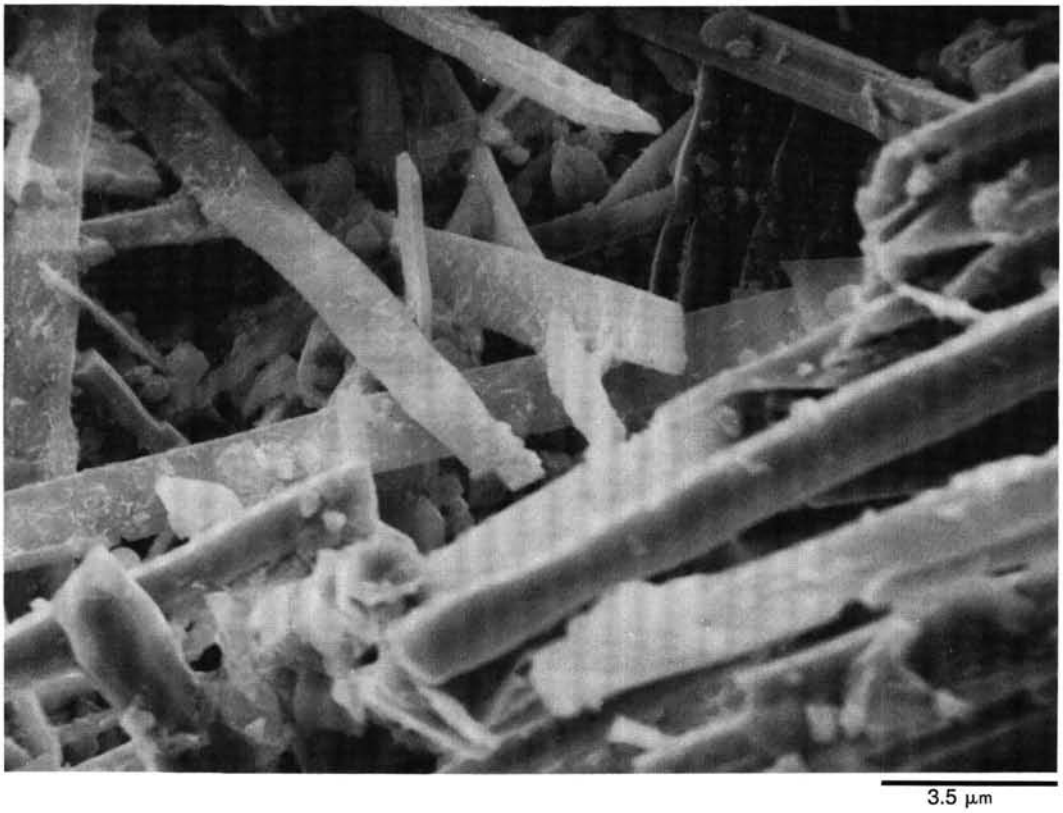

Figure 9. Bladed habit of some of the aragonite in Figure 8 SEM photograph. Apparent undulations in some crystal edges are due to ship's motion.

hydroxyoxides lining some of the vesicles and most of the miarolitic cavities. At one end of the sample, a lighter gray, fresher-looking, irregular oval patch about 3–4 cm across is enclosed entirely within the dark-gray zone. The minimum distance between the light/dark contact and the exterior of the sample is 5 mm.

Two thin sections of this sample were made from the routinely taken minicore, which was entirely from the dark-gray zone. The general appearance of the rock in thin section is fresh. No birefringent clays occur. The only visible alteration products are a yellow, transparent, isotropic "clay," poorly reflective in reflected light, and a dark-red, isotropic, higher relief, moderately reflective iron-hydroxyoxide. Of these, the yellow material is much the more abundant and occurs mainly as miarolitic linings and fillings and as vesicle linings. The red iron-hydroxyoxide occurs in the same textural sites as does the yellow material. Where both occur together, the yellow material overgrows the iron-hydroxyoxide. The distribution of these alteration products in the sections is heterogeneous, but no distinct alteration domains are apparent.

Little indication of replacive alteration exists. The mesostasis is microcrystalline and appears fresh in reflected light, apart from some angular pitting that might represent minor hydrated glass. A few primary sulfide globules are observed. Their scarcity may or may not indicate that some of the original sulfide has been oxidized.

Alteration Products Coating the Rock

The exterior of the sample (including any vesicles exposed at the surface) has various types of secondary coating, some of which resemble the coatings on Piece 1:

1. Very thin, homogeneous dull olive-green coatings, probably smectite (as in Piece 1).
2. Dull orange-red coatings, locally microscopically botryoidal, probably iron-hydroxyoxide.
3. Rusty red to pale-orange patchy coating, accompanied by scattered "micromanganese nodules."

In addition to these coatings, a crack running across the drilled surface of the archive half has controlled the deposition of a pale-yellow to cream-colored, locally rusty-stained soft clay(?) mineral, accompanied by aggregates of black MnO_2(?) as much as 0.3 mm across. Whether these materials constitute a fracture-filling within the rock or merely a localized surficial deposit, similar to that described from Piece 1, is unclear.

X-Ray Diffractometry

A small amount of the soft, orange to cream-colored external alteration material coating Piece 1 was scraped off and mounted on a glass slide for XRD. No reliable peaks other than the strongest lines of plagioclase were obtained. This result probably reflects the inadequate sample volume rather than any characteristic of the material. A small thin-section billet-sized piece was sawn from a dark halo in Piece 1, and a "clay concentrate" was prepared from it and run on the XRD as described in the Site 648 chapter "Alteration" section (this volume). More clay was separated from this sample than from the Hole 648B samples, yet the clay peaks obtained were broad and of low intensity (Fig. 10). This was at least in part due to flocculation of the clay into unoriented aggregates as the suspension dried on the slide. The observed clay peaks (Table 4) indicate that the principal alteration phase (as in Hole 648B) is smectite.

Summary and Interpretation

A tentative sequence of alteration stages can be reconstructed for the Site 669 samples. Piece 1 probably became a detached clast while still almost fresh. As part of a rubble pile, it was altered in similar fashion to the Site 648 samples, developing a type 1 dark halo. A thin oxidized coating, including "micromanganese nodules," developed on the exterior, and solutes (from this oxidation and alteration of other rubble pieces and/or from seawater) entered the halo zone, initiating precipitation of significant amounts of smectite and minor amounts of iron-hydroxyoxides, mainly as miarolitic fillings. The presence of large, irregular vesicles permitted the precipitation of some secondary minerals within the otherwise fresh interior. Green clay (smectite?) precipitated along cracks in the samples, but no dark halos developed parallel to these cracks. In time, the voids between the rubble pieces became filled with calcareous sediment. This provided a source of $CaCO_3$ and probably a high-pH environment that allowed aragonite to precipitate in voids. The sediment may also have inhibited further oxidative alteration because the dark halo has not advanced as far as the type 2 halos in Hole 648B, where the rocks are much younger.

Piece 2, less comprehensively studied than Piece 1, appears to have had a sequence of alteration stages similar to Piece 1, but the dark halo has advanced to a Hole-648B-type-2 state. Most of the altered zone is of a clay-poor oxidized type mineralogically resembling the light zones of Hole 648B type 2 halos but is dark, perhaps because of the fine grain size. Whether a clay-rich band exists between this type of alteration and the apparently fresh interior zone is unclear. No aragonite occurs in Piece 2.

Both pieces from Site 669 show no alteration of primary silicate minerals, despite their greater age (1–2 m.y.) than Site 648.

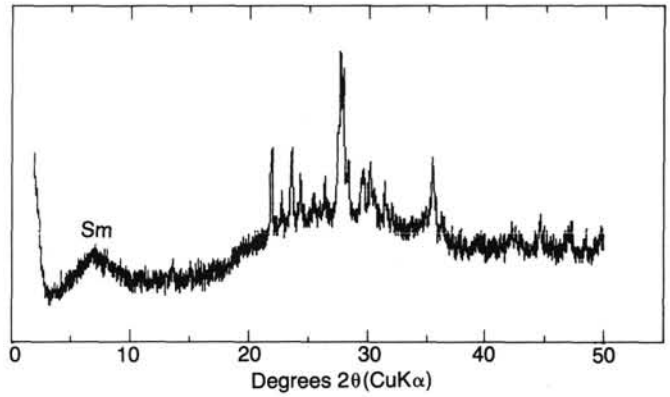

Figure 10. X-ray diffractogram of air-dried clay concentrate from dark alteration halo in Sample 109-669A-1D-1, 4–6 cm. Sm = smectite. Other peaks assignable to plagioclase (cf. Site 648 chapter, "Alteration" section, Fig. 41, this volume).

Table 4. X-ray diffraction results. Listing of all recorded peaks with d-spacings >3.5 angstroms. Peak quality is defined in Table 10 of Site 648 chapter "Alteration" section (this volume).

Sample	d-spacing	I/I_{max} (%)	Peak quality	Assignment
109-669A-1D-1	12.3	18.7	1.58	Smectite
4–6 cm	6.47	15.5	1.12	Plagioclase
Halo	4.58	48.6	0.76	Smectite
(air)	4.04	96.2	0.89	Plagioclase
	3.90	49.4	0.76	Plagioclase
	3.76	100	2.24	Plagioclase
	3.64	63.0	1.35	Plagioclase
109-669A-1D-1	17.2	18.5	1.07	Smectite
4–6 cm	6.48	13.7	1.15	Plagioclase
Halo	4.05	100	1.07	Plagioclase
(glycol)	3.90	45.3	1.32	Plagioclase
	3.76	74.1	0.98	Plagioclase
	3.64	48.6	1.82	Plagioclase

PHYSICAL PROPERTIES

A physical-properties sample was obtained from the largest piece of basalt recovered from Hole 669A, and bulk and grain density, porosity, and ultrasonic compressional velocity were determined using standard shipboard techniques. The techniques are described in the Site 648 chapter "Physical Properties" section (this volume).

Results

For Sample 109-669A-1D-1, 11–13 cm, the values are as follows (numbers in parentheses represent the range in the measurements):

Wet weight: 27.485 g (average of two measurements)
Dry weight: 26.92 g (average of two measurements)
GRAPE wet-bulk density: 2.866 g/cm^3 (±0.015)
GRAPE dry-bulk density: 2.814 g/cm^3 (±0.035)
Ultrasonic velocity:
  Saturated: 5.59 km/s (± 0.1)
  Dry: unreliable
Sample volume: 9.590 cm^3
Porosity: 5.8%
Grain density: 2.978 g/cm^3

These results are within the range of expected values for oceanic basalts (e.g., Hyndman et al., 1984; Salisbury et al., 1985). The compressional velocity is somewhat higher than that measured on samples from Hole 648B, but the density and porosity are essentially the same. In fact, this sample has a somewhat higher porosity than does the nonvesicular Hole 648B basalts.

The average grain size is smaller in this sample than in samples from Hole 648B. Furthermore, although only a few small vesicles are visible in hand specimen, many small (<0.2 mm), irregular vesicles can be seen under the microscope. In contrast to the samples from Hole 648B, no evidence exists of a significant component of groundmass porosity. Theoretical results suggest that velocity is less sensitive to equidimensional porosity than to an equivalent amount of crack porosity (e.g., O'Connell and Budiansky, 1974; Toksoz et al., 1976). This implies that the porosity (which is primarily vesicular) does not greatly affect velocity; the absence of a significant component of low-aspect-ratio intergranular porosity results in a much higher compressional velocity than in the somewhat less porous Hole 648B rocks. However, a determination of shear velocity would be required to confirm this explanation.

THERMAL CONDUCTIVITY

The thermal conductivity of one basalt sample recovered from Hole 669A was measured using the Thermcon half-space needle device as outlined in detail in the thermal-conductivity section ("Site 648" chapter, this volume). Table 5 shows the results of the measurements. The mean value of 1.76 W/m·°C is within the variation of the thermal conductivities measured on the basalt samples from Hole 648B.

Table 5. Results of thermal-conductivity measurements on basalt sample from Hole 669A.

Core section	Distance from top of section (cm)	Thermal conductivity (W/m·°C)
109-669A-1D-1	0–10	1.76 (1.71)
		1.77 (1.77)
		1.75 (1.63)
		1.76 (1.70)

SUMMARY AND CONCLUSIONS

We successfully spudded-in and established a 4.0-m-deep hole in intermixed sediment and basalt rubble, but the PDCM obviously did not have enough power to actually penetrate the presumed gabbroic basement. Clearly, technological improvements and more experience are needed to test the feasibility of penetrating and coring gabbro outcrops.

The two pieces of aphyric basalt recovered from the rubble cover are tholeiitic basalts, similar to some of the olivine phyric basalts collected from the walls of the Kane Fracture Zone, and show evidences of incipient alteration characterized by the "dark halos" stage (mainly orange smectites, green to yellow clays, and iron-hydroxyoxides). Aragonite crystals were found in some vesicles and miaroles.

REFERENCES

Bryan, W. B., 1972. Morphology of quenched crystals in submarine basalts. *J. Geophys. Res.*, 77:5812–5819.

Bryan, W. B., Thompson, G., Frey, F. A., and Dickey, J. S., 1976. Inferred settings and differentiation in basalts from the Deep Sea Drilling Project. *J. Geophys. Res.*, 81:4285–4304.

Bryan, W. B., Thompson, G., and Ludden, J. N., 1981. Compositional variation in normal MORB from 22°–25° N.: Mid-Atlantic Ridge and Kane Fracture Zone. *J. Geophys. Res.*, 86:11,815–11,836.

Detrick, R. S., Ryan, W. B., Mayer, L., Fox, P. J., Kong, L., Manchester, K., Kastens, K., Karson, J., and Pockalny, R., 1985. Mid-Atlantic Ridge/Kane Fracture Zone final site survey report. *Joint Oceanographic Institutions.*

Hyndman, R. D., Christensen, N. I., and Drury, M. J., 1984. The physical properties of basalt core samples from Deep Sea Drilling Project Leg 78B, Hole 395A. *In* Hyndman, R. D., and Salisbury, M. H., et al., *Init. Repts. DSDP*, 78: Washington (U.S. Government Printing Office), 801–810.

Karson, J. A., and Dick, H.J.B., 1983. Tectonics of ridge-transform intersections at the Kane Fracture Zone. *Mar. Geophys. Res.*, 6:51–98.

MacKenzie, W. S., Donaldson, C. H., and Guilford, C., 1982. Atlas of igneous rocks and their textures. New York (Wiley).

O'Connell, R. J., and Budiansky, B., 1974. Seismic velocities in dry and saturated cracked solids. *J. Geophys. Res.*, 79:5412–5426.

Salisbury, M. H., Christensen, N. I., Becker, K., and Moos, D., 1985. The velocity structure of Layer 2 at Deep Sea Drilling Project Site 504 from logging and laboratory experiments. *In* Anderson, R. N., Honnorez, J., and Becker, K., et al., *Init. Repts. DSDP*, 83: Washington (U.S. Government Printing Office), 529–539.

Tarney, J., Saunders, A. D., Weaver, S. D., Donellan, N.C.B., and Hendry, G. L., 1979. Minor-element geochemistry of basalts from Leg 49, North Atlantic Ocean. *In* Luyendyk, B. P., Cann, J. R., et al., *Init. Repts. DSDP*, 49: Washington (U.S. Govt. Printing Office), 657–691.

Toksoz, N., Cheng, C. H., and Timur, A. 1976. Velocities of seismic waves in porous rocks. *Geophysics*, 41:621–645.

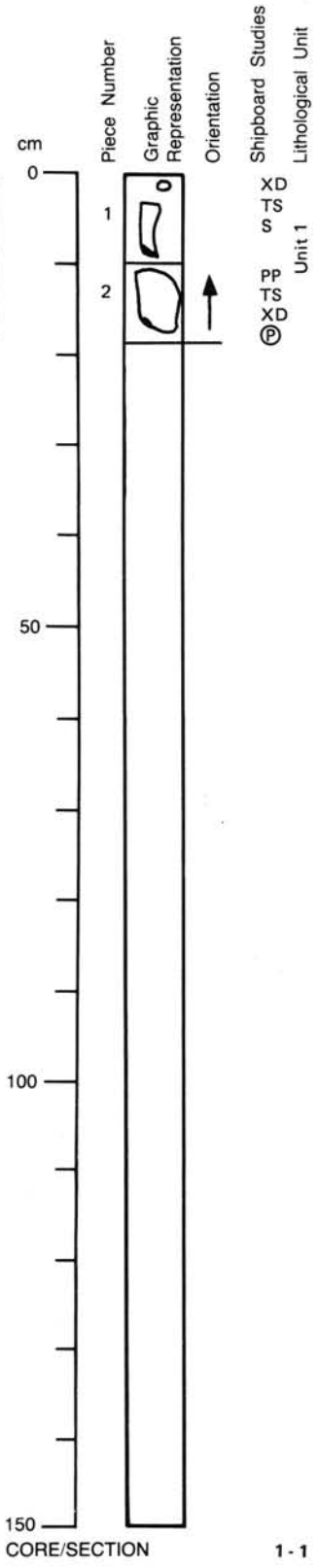

109–669A–1D–1

UNIT 1: ASSORTED RUBBLE

Pieces 1–2: APHYRIC BASALT

GLASS: None, no contacts.
PHENOCRYSTS: Piece 2: One plagioclase phenocryst near lower edge.
Plagioclase – 1%, 2 mm, euhedral, fresh.
GROUNDMASS: Uniformly fine grained.
COLOR: Gray.
VESICLES: 2–3%, 0.2–1.0 mm, round, empty, filled with microcrystalline groundmass, or lined by bluish smectite in alteration halos, homogeneous distribution.
Miaroles: Approximately 25% of all voids, 0.1–0.5 mm, sub-circular to elongate-irregular, empty or lined by bluish smectite in alteration halos, homogenous distribution.
ALTERATION: Fresh to slightly altered.
Piece 1: Dark alteration halo 2–4 mm wide developed parallel to edges; vesicles lined with bluish smectite, iron oxide/clay mixture, yellow brown clay and zeolites; edges coated with yellow brown clay and zeolites.
Piece 2: Dark alteration halo 2–25 mm wide developed around outside of sample, vesicles lined with bluish smectite.
VEINS/FRACTURES: Piece 2 contains crack filled with yellow clay.

THIN SECTION DESCRIPTION

109-669A-1D-1 (Piece 1, 7-9 cm)

ROCK NAME: Aphyric basalt

WHERE SAMPLED: Unit 1, pillow or flow interior, cut perpendicular to dark halos

TEXTURE: Variolitic to microlitic

GRAIN SIZE: Fine

PRIMARY MINERALOGY	PERCENT PRESENT	PERCENT ORIGINAL	SIZE RANGE (mm)	APPROX. COMPO-SITION	MORPHOLOGY	COMMENTS
PHENOCRYSTS						
Olivine	Tr	Tr	0.3–0.6		Subhedral	
GROUNDMASS						
Plagioclase	29	29	51		Acicular, bunches	Radiating. Associated with rare ol nucleus of plag. L/W = 10–30.
Olivine	3	3	0.05–0.2		Euhedral, skeletal	Generally attached to plag.
Clinopyroxene	11	11	<0.1		Radiating, plumose	Rare small grain associated with radiating plag.
Mesostasis	54	54				Product of glass devitrification. Rare euhedral crystals.
Opaques	0.5	0.5	3–10m	Magnetite	Anhedral–euhedral	Dark brown, isotropic with plag and cpx crystallites. Tiny grains distributed in the mesostasis.

SECONDARY MINERALOGY	PERCENT	REPLACING/ FILLING	COMMENTS
Clays	2	Mesostasis	Yellow birefringent clay.
Carbonate	Tr	Miaroles	Aragonite, radiating. SEM photo taken before sectioning.
Fe hydroxide	0.5	Mesostasis	Both red and opaque varieties.

HALO ZONE 34 mm wide

Yellow Clay	Strongly colored. Almost cryptocrystalline. Low birefringence. Occurs mainly as homogeneous partial fillings of miaroles. These fillings are up to 3.5 mm in extent, with groundmass plag, cpx, ol, and titanomagnetite projecting into the clay. Clay has botryoidal, locally radiate growth structure. The same clay also forms partial replacements of brown mesostasis–(?)glassy component. Replacement of mesostasis occasionally nearly complete.
Orange–red clay	Trace amounts, mainly as miarole lining. Transitioned between yellow clay and red Fe hydroxide.
Red Fe hydroxide	Occurs mainly in fractures, lining vesicles and forming the central parts of miarole fillings. Vesicle linings up to 50m. Cracks < 10m wide locally spaced at 100m intervals. Occasionally occurs as 330–50m grains attached to miarole walls, then overgrown by yellow clay. In one case, a bleb of Fe hydroxide attached to a miarole wall is continuous with a 31m thick Fe hydroxide veinlet.
Opaque Fe hydroxide	Occurs as central parts of two or three miarole linings.
Point count of halo zone:	26 yellow clay (5%), 7 red Fe hydroxides (1.5%), 1 opaque Fe hydroxide (Tr), 466 primary phases.
CENTRAL ZONE (fresh)	Traces of orange to red Fe hydroxide, mainly near vesicle walls. Radiating aggregates of aragonite (biaxial, low 2V, extreme birefrigence) in large (5 mm), irregular miarole (also containing hopper ol). This and a smaller aragonite-filled miarole are in fact in connection with the halo zone.

VESICLES/ CAVITIES	PERCENT	LOCATION	SIZE RANGE (mm)	FILLING	SHAPE	COMMENTS
Vesicles	1.5	Even	0.2–0.8		Rounded to irregular	Miaroles in alteration halos more commonly filled with clays than the vesicles. Empty in fresh mesostasis.

COMMENTS: *Rare ol phenocrysts are rather microphenocrysts. Mesostasis is cryptocrystalline to microcrystalline with plag, cpx, and ol microlites.* This section might represent a coarser equivalent of Section 669A-1D-1 (Piece 2, 11–13 cm).

THIN SECTION DESCRIPTION

109-669A-1D-1 (Piece 2, 11-13 cm)

ROCK NAME: Aphyric basalt
WHERE SAMPLED: Unit 1, pillow or flow interior
TEXTURE: Intergranular (felty)
GRAIN SIZE: Microcrystalline to fine

PRIMARY MINERALOGY	PERCENT PRESENT	PERCENT ORIGINAL	SIZE RANGE (mm)	APPROX. COMPO-SITION	MORPHOLOGY	COMMENTS
PHENOCRYSTS						
Olivine	0.5	0.5	0.2-0.4		Euhedral-subhedral	Some embayment. Some glass inclusions.
GROUNDMASS						
Olivine	5	7	<0.1		Euhedral, quenched morphologies	Radiating, swallow tail.
Plagioclase	26	26	<0.1		Acicular, Hopper-shape	Radiating, spherulites.
Clinopyroxene	39	40	0.1-0.3		Anhedral, plumose	Christmas-tree texture, product of glass devitrification.
Mesostasis	21	21				Dark brown with some cpx and plag crystallites.
Opaques	4.5	5.5	<<0.1	Magnetite, sulfides	Anhedral	Very minute grains in mesostasis or cpx.
Segregation vesicule	Tr	Tr	0.2-0.5		Rounded	Mostly devitrified glass.

SECONDARY MINERALOGY	PERCENT	REPLACING/ FILLING	COMMENTS
Clays	3	Vesicles, miaroles, ol, cpx	Yellow. Replaces olivine and clinopyroxene (staining).
Fe hydroxide	1	Opaques	Reddish brown to red. Individual granules.

VESICLES/ CAVITIES	PERCENT	LOCATION	SIZE RANGE (mm)	FILLING	SHAPE	COMMENTS
Vesicles, miaroles	2	Even	0.2-0.4	Clays, Fe hydroxide	Rounded or irregular	Can be empty or lined.

THIN SECTION DESCRIPTION

109-669A-1D-1 (Piece 2, 11-13 cm)

ROCK NAME: Aphyric basalt
WHERE SAMPLED: Unit 1, pillow or flow interior
TEXTURE: Spherulitic to variolitic
GRAIN SIZE: Microcrystalline

PRIMARY MINERALOGY	PERCENT PRESENT	PERCENT ORIGINAL	SIZE RANGE (mm)	APPROX. COMPO-SITION	MORPHOLOGY	COMMENTS
PHENOCRYSTS						
Olivine	Tr	Tr	~2.5		Anhedral	Yellow hydroxide attached to the phenocryst.
GROUNDMASS						
Plagioclase	34	35	<0.6		Bundles, hopper, acicular	Radiating. Associated with cpx or attached ol. Nucleus of plag.
Olivine	6	6	<0.1		Euhedral, swallow tail	Attached to plag.
Clinopyroxene	33	33	<0.4		Radiating, plumose	Christmas tree-shape. Forms spherulites with plag or in the mesostasis.
Mesostasis	22	24				Dark brown, isotropic. Investigation under reflected light reveals plag and cpx crystallites.
Opaques	2	2	μ's	Magnetite	Anhedral	Minute grains distributed in the mesostasis only.

SECONDARY MINERALOGY	PERCENT	REPLACING/ FILLING	COMMENTS
Fe hydroxide	2	Vesicles, mesostasis	Yellow to reddish brown. Associated with plag, cpx, and ol or randomly distributed in the groundmass. The granules are attached to the crystals or interfingered with cpx.

VESICLES/ CAVITIES	PERCENT	LOCATION	SIZE RANGE (mm)	FILLING	SHAPE	COMMENTS
Vesicles	2	Even	0.05-0.8 .8	Fe hydroxide	Irregular	Only partially filled. Surrounded by opaque mesostasis, darker than usually observed away from the vesicles.

COMMENTS: Ol phenocrysts are in fact microphenocrysts. These are, however, different from quenched ol grains. Mesostasis is cryptocrystalline with recognizable cpx and plag in a radiating pattern. Segregation vesicles consisting of minute crystals of plag + cpx + cryptocrystalline material constitute approximately 1% of the rock.